Available online at www.sciencedirect.com
SCIENCE DIRECT
Vibrational Spectroscopy 38 (2005) 169–177
VIBRATIONAL SPECTROSCOPY
www.elsevier.com/locate/vibspec

Microspectroscopy of single proliferating HeLa cells

Susie Boydston-White [a,*], Tatyana Chernenko [a], Angela Regina [a], Miloš Miljković [a,b], Christian Matthäus [a,b], Max Diem [a,b]

[a] Department of Chemistry and Biochemistry, Hunter College of the City University of New York, 695 Park Avenue, New York, NY 10021, USA
[b] PhD Program in Chemistry, The Graduate School and University Center, City University of New York, 365 Fifth Avenue, New York, NY 10016, USA

Received 3 December 2004; accepted 14 February 2005
Available online 13 June 2005

Abstract

Spectral differences between normal and abnormal tissue observed to date appear to be due to different averaging processes of spectral patterns that differ according to the cell's biochemistry, due to its state of maturation, differentiation, and development. Thus, disease perturbs the distribution of cells in the different stages of maturation, differentiation, and development. Previous FTIR microspectroscopic studies of normal versus neoplastic cells and tissues have demonstrated differences in the absorption intensities and band-shapes, particularly in the low frequency (1200–1000 cm^{-1}) spectral region. In this study, we further investigated the spectral changes due to the drastic biochemical and morphological changes occurring as a consequence of cell proliferation.

Keywords: Microspectroscopy; Tissue; HeLa cells; Cell cycle; FTIR micro-spectroscopy; Cell division

1. Introduction

Whether considering the environment of a single-celled organism or that of a single cell in a multicellular organism, each individual cell is a complex web of biochemical reactions. A multicellular organism has the same genetic material in nearly every cell, yet has more than 200 different types of cells – each type having a different shape, size and functionality – with all these cells having descended from a single cell.

Whether as part of an animal or grown in culture, living cells are either growing or quiescent. Although an increase in the size of a cell plays a role in the growth of organs and tissues, an increase in the number of cells is by far the most important factor in both normal and abnormal growth. Cells can grow without dividing by absorbing more liquid or by manufacturing larger concentrations of intracellular protein. However, once a critical size has been reached, and/or if an appropriate signal has been received, most somatic cells will initiate processes that lead to cell division [1]. In preparation for cell division, the mass of the ''parent'' cell must double and all of its subcellular organelles (i.e., mitochondria, golgi bodies, etc.) must be exactly duplicated to insure that each ''daughter'' cell has the same functional potential as the parent. After cell division is completed, each of the identical daughter cells must contain not only exact copies of the parent cell's DNA, but the replicated chromosomes must have been correctly segregated. Thus, to understand the growth, differentiation and development of both normal and abnormal cells and tissues, it is appropriate to review in further detail the structures and regulatory processes relevant to the normal eukaryotic somatic cell cycle.

Cell proliferation is important to understand because the vast majority of cell types in the human body do not divide regularly, yet every cell – with a few notable exceptions – has the capacity to proliferate in response to an external signal or in response to an internal event. A quiescent (or G0) somatic cell is one that is not increasing its mass or passing through the cell division cycle. These cells carry out the characteristic functions of tissues, such as the synthesis of export proteins in the liver or the transmission of impulses in a nerve. A normal G0 cell is potentially able to proliferate, but has left the cell

* Corresponding author.

0924-2031/$ – see front matter © 2004 Elsevier B.V. All rights reserved.
doi:10.1016/j.vibspec.2005.02.028

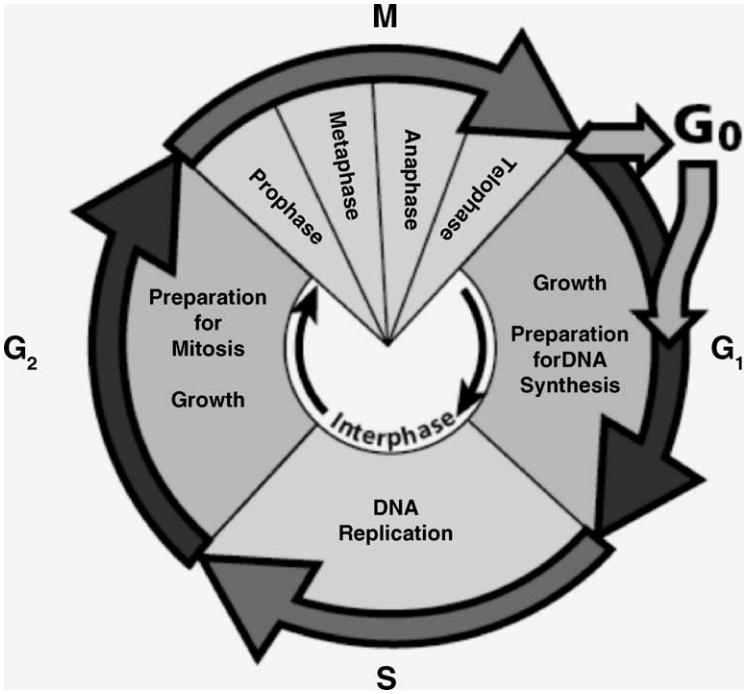

Fig. 1. The eukaryotic cell cycle.

cycle and remains dormant until an appropriate stimulus triggers its reentrance to the cell division cycle.

Once such a signal is received, a cell enters the cell division cycle, for which the major phases are shown in Fig. 1. The eukaryotic cell cycle is defined as the interval of time between the completion of mitosis (physical division of the cell) in the parent cell and the completion of mitosis in one or both of the daughter cells. Cell-cycle lengths vary considerably in the tissues of living organisms [2]. When human cells are grown in vitro, many cell types generally exhibit a cycle length of around 24 h [3]. For cycling cells, the cell cycle is divided into four main phases:

1. *G1 phase*. After completion of mitosis, this is the first resting, or ''gap'' phase,
2. *S phase*. The phase in which DNA synthesis produces an exact copy of the chromosomal DNA,
3. *G2 phase*. A second resting or ''gap'' phase, and
4. *M phase*. The mitotic phase, where the cell physically divides; within this phase there are also several subphases.

In order to develop spectroscopic techniques for diagnosing disease, we have studied the IR spectral differences between resting and dividing cells [4], because we have evidence that the distinction between normal and diseased tissues is closely coupled to the understanding of spectral features of resting and dividing cells [5]. This leads to the study of the cell-cycle-dependent differences in the FTIR micro-spectral features of single cells.

In order to study the cell-cycle dependence of the spectra, we must first separate a healthy, proliferating population of cultured cells into populations of pure or highly enriched for each of the cell-cycle phases without harming the cells or perturbing their internal biochemistry. Chemical and physical whole-culture synchronization methods have been used for many years in the field of cell biology to enrich cell cultures for cell-cycle phase in order to study events during the cell cycle and are accepted as valid approaches to cell-cycle analysis [6]. Physical methods for whole-culture synchronization include centrifugal elutriation and mitotic shake-off (mitotic selection). Since we are studying the cell-cycle dependence of the FTIR spectra of single cells to determine the spectral patterns of individual cells as a function of its state of development, we must forego any chemical treatments leading to cell-cycle arrest due to the biochemical perturbations. Instead, we must employ a physical method for enriching cultured cell populations for cell-cycle phase.

In this study, we report results of following cells for about 24 h after mitotic shake-off (described below). In order to achieve unambiguous identification of the stage within the cell cycle, we employ a number of immunohistochemical procedures that are specific for the stage within the cell cycle.

2. Materials and methods

2.1. Cell culture

Cells from the cervical adenocarcinoma cell line HeLa cells (ATCC CCL-2) were seeded in five 75 cm^3 sterile plastic cell culture flasks (Fisher) at a concentration of about 2×10^4 cells/cm^2 in 20 mL Dulbecco's modified

Eagle's medium (DMEM) (ATCC), with 2.5 μg/mL of amphotericin B (ATCC), 100 IU/mL penicillin/streptomycin (ATCC), supplemented with 10% fetal bovine serum (FBS) (ATCC) and incubated at 37 °C and 5% CO_2 until the cells reached 50% confluence. At this time, the medium was removed, the cells rinsed in sterile 1× phosphate buffered saline (PBS) (ATCC) and 15 mL fresh medium was added, sans amphotericin B. The cells were incubated overnight.

2.2. Mitotic detachment

"Mitotic detachment" or "mitotic shake-off" is a widely used cell biology technique that has been around since 1961 to synchronize cells in culture [7]. This physical separation technique makes use of the fact that adherent mammalian cells in culture attach themselves firmly to the cell culture container while in interphase (G1, S or G2). Fig. 2, for example, shows an asynchronously growing population of HeLa cells adhering to a low-e slide. The attachment is so firm that removal of an interphase cell from the culture container requires treatment of the cells by the protease trypsin to partially digest the cell-surface proteins responsible for the attachment. However, during the very short M phase, the cells "round up" and detach almost completely from the surface of the culture container. Applying a brief vibration to the culture container is enough to harvest mitotic cells such that we may select only cells in the M phase and follow them through a time course of about 24 h.

Mitotic shake-off was carried out as follows. The culture medium was removed and 20 mL of 1× PBS was added to each flask. The flasks were "shaken" on a laboratory vortex mixer on a medium-high setting for 45 s to remove debris, poorly adherent and dead cells. The PBS was removed and replaced with 15 mL of fresh, warmed DMEM supplemented with 10% FBS. The flasks were returned to the incubator and allowed to incubate for 1 h. After incubation, the flasks were each again "shaken" for 45 s on the vortex mixer and the medium immediately removed and added to a sterile 15 mL falcon tube. The tubes were centrifuged for 6 min at 80 × *g* to collect the cells. The pellets were re-suspended in warmed DMEM culture medium to a total volume of 1.5 mL.

Fig. 2. Adherent HeLa cells grown on a low-e slide. This view represents an approximately 250 μm wide view at 40× magnification.

2.3. Post-mitosis incubation

Ten 100 mm × 100 mm square polystyrene sterile Petri dishes (Fisher), were prepared, each with three low-e slides (see below) immersed in 25 mL DMEM, supplemented with 100 IU/mL penicillin/streptomycin and 10% FBS. The re-suspended mitotic HeLa cells were pipetted onto the slides at 50 μL per slide. The dishes were allowed to sit undisturbed for 5 min to allow the cells to settle onto the slides. The Petri dishes were then placed in the incubator at 37 °C and 5% CO_2. After 30 min, one slide was carefully removed for S-phase labeling (see below). Slide removal was repeated each hour for 30 h. Since the cells were viable, these slides represent a time course of the cells over 30 h after the initial mitotic division.

Due to the variability of the length of each individual cell's cell cycle, elapsed time following mitosis is not enough information to ensure the biochemical age of a proliferating cell, which must be confirmed by additional means. We employed immunohistochemical staining for specific cellular events, including the appearance (and subsequent disappearance) of cyclin E and cyclin B1 and the uptake and incorporation of the thymidine analog 5-bromo-2′-deoxyuridine (BrdU) into nascent DNA during synthesis. The former two methods can be employed after cells have been fixed and dried, whereas the BrdU uptake must be performed with the live cells [8].

2.4. 5-Bromo-2′-deoxyuridine labeling (BrdU)

Once a slide was removed from a Petri dish, it was immediately transferred under sterile conditions to a Petri dish containing 25 mL DMEM, supplemented with 100 IU/mL penicillin/streptomycin, 10% FBS and 50 μM BrdU (EMD Biosciences) and incubated at 37 °C and 5% CO_2 for 30 min [9,10].

2.5. Fixation

After 30 min BrdU incubation, each slide was removed from the medium and washed with 1× PBS. The slide was then placed in a 50 mL falcon tube (Fisher) containing 40 mL 10% buffered formalin solution (Sigma) for 30 min at room temperature. Each slide was fixed in this manner.

2.6. Preparation for FTIR

After fixation, each slide was removed from the buffered formalin solution and placed in a Coplin staining jar containing 1× PBS for 1 min at room temperature. The slide was then placed in a Coplin jar containing Hank's buffered saline solution (HBSS) (ATCC) for 1 min at room temperature. Once each slide was removed from the HBSS, to prevent the formation of salt crystals on the slide as it dries, it was doused with Millipore water. The water was quickly removed by spraying the slide gently with compressed air. After washing and brief air-drying, each slide was placed in a desiccator for overnight drying at room temperature.

2.7. FTIR microspectroscopy

After visual evaluation, a grid was applied to the reverse of the slide to aid in locating cells when using different microscopes. The slides were placed on the stage of the Perkin-Elmer Spectrum One/Spotlight 300 IR Spectrometer. Pairs of cells, in close proximity to each other and nearly identical in size, were visually located, indicating a harvested mitotic cell that had survived handling and subsequently divided and attached to the slide. The FTIR reflectance – absorbance spectra were collected in point mode using various aperture sizes to accommodate the different cell shapes and sizes. The digital stage location was correlated with the applied grid. A spectrum for the entire HeLa cell (full-cell spectrum) was taken by co-adding 64 interferograms at 4 cm^{-1} spectral resolution. The aperture was then adjusted (closed) to include only the cell nucleus and a spectrum for just the nucleus was collected separately, co-adding 64 interferograms. Then, a visible image was collected for each cell pair.

2.8. Data manipulation

Using Grams/AI 7.01 (Thermo Galactic), the full-cell spectra were baseline-corrected, vector normalized to the absorbance intensity of the amide I peak, smoothed using a Savitzsky-Golay smoothing algorithm and truncated to a range of 1800–900 cm^{-1}. The spectra taken from at least 10 cells from each slide were averaged to produce the average spectrum for each post-mitosis hour time point. The second derivative spectrum was also calculated for each of the spectra taken on each slide. These second derivative spectra were averaged to produce the average second derivative spectrum for each time period. The above manipulations were repeated on the nuclear spectra to yield an average spectrum and an average second derivative spectrum for each time point post-mitosis.

2.9. Immunostaining

After infrared data acquisition, the slides were subjected to immunohistochemical staining. The staining consisted of three primary antibodies: rat monoclonal anti-5-bromo-2′-deoxyuridine (BrdU) conjugated with fluorescein isothiocyanate (FITC) (Abcam), mouse monoclonal anti-cyclin B1 (Abcam) and rabbit polyclonal anti-cyclin E (Abcam) and two secondary antibodies: goat polyclonal anti-mouse conjugated with Alexa Fluor 360® (Molecular Probes) and goat polyclonal anti-rabbit IgG conjugated with Texas Red® (Calbiochem).

The anti-BrdU, anti-cyclin B1 and anti-cyclin E primary antibodies were diluted 1:150 in a buffer solution of 60 mM Tris (Sigma), 0.6 mM magnesium chloride (Sigma), 1 mM 2-mercaptoethanol (Sigma), 2% bovine serum albumin (BSA) (Sigma) and 2 U/μL DNase I (Sigma). The slides were covered with a 1× PBS solution for 30 min at 37 °C to rehydrate the cells. Once the PBS was removed from the slides, a solution of 0.2% Triton X-100 (Sigma) in 1× PBS was pipetted onto the slides to permeabilize the cells. The cells were permeabilized for 3 min, then washed twice for 1 min in a solution of 0.02% Tween 20 (Sigma) and 0.04% sodium azide (Sigma) in 1× PBS (PBST). A blocking solution of 2% BSA in PBST was pipetted onto the slides. About 200 μL was needed to cover the cells. The slides were incubated at room temperature for 10 min. The blocking solution was removed and 200 μL of the primary antibody solution was pipetted onto the slides. The cells were incubated in the primary antibody solution at 37 °C for 1 h.

After primary antibody incubation, the slides were washed in PBST three times for 3 min. The secondary antibody solution was prepared by diluting the two secondary antibodies 1:500 in a 2% BSA in PBST solution. After washing, 200 μL of the secondary antibody solution was pipetted onto the slides. The slides were incubated at 37 °C in the dark for 1 h. Upon completion of secondary antibody incubation, the slides were washed five times for 5 min in PBST, then for 1 min in HBSS.

To aid in identifying the limits of the cell nucleus during fluorescence microscopy, the slides were then counterstained with 4′,6-diamidino-2-phenylindole, dihydrochloride (DAPI) at a concentration of 0.2 μg/mL at room temperature for 3 min. After counterstaining, the slides were washed three times in BSS, then doused briefly with Millipore water. The water was quickly removed by spraying the slide with compressed air and allowed to air dry in the dark.

2.10. Fluorescence microscopy

Using the grid affixed to the underside of the slide, the cells for which spectra had been collected were located on the slide. The fluorophores were visualized via a Nikon Optiphot-2 microscope. This fluorescence microscope is equipped with a mercury lamp and an episcopic-fluorescence attachment EFD-3, utilizing appropriate excitation and emission filters for the FITC and Texas Red® fluorophores, as well as a multi band filter block for visualizing the Alexa Fluor® emission. For FITC the sliding filter block is equipped with an excitation filter that allows

for an excitation of 465–490 nm, a dichroic mirror at 505 nm and a barrier filter that allows for an emission of 515–555 nm. For Texas Red®, the sliding filter block is equipped with an excitation filter that allows for an excitation of 540–580 nm, a dichroic mirror at 595 nm and a barrier filter that allows for an emission of 600–660 nm. The FITC, Alexa Fluor® and Texas Red® fluorescence images were acquired using the Plan Apo DIC 60× oil objective and the attached Sony camera. The images were manipulated using Micrografx Picture Publisher version 8.

3. Results

After staining for incorporated BrdU (green fluorescence), cyclin E (red fluorescence) and cyclin B1 (yellow fluorescence), the fluorescence images of the cell pairs were matched via the attached grid with the visible images collected during the FTIR microspectroscopy. Fig. 3 shows four time periods and the typical cell pair with its staining pattern that was found to be typical for the cell pairs populating that slide. Since the thymidine analog BrdU is integrated into nuclear DNA only during the S-phase, the positive green staining for BrdU indicates that the cell was actively synthesizing DNA at the time of BrdU incubation. Positive red staining for cyclin E indicates that the cells contained sufficient quantities of cyclin E for detection at the time they were fixed. Cyclin E is a nuclear protein synthesized only in proliferating cells and only during the G1 phase [11]. Cyclin E reaches its maximum concentration at the end of G1 and is quickly degraded during the early S phase [10]. Cells that exhibit a double-staining positive for both incorporated BrdU and cyclin E are in the early stage of the S phase when they were fixed [11]. Positive yellow staining for cyclin B1 indicates that the cell contained sufficient quantities of cyclin B1 for detection. Cyclin B1 is a cytoplasmic protein synthesized only in proliferating cells and only in the G2 phase [11]. The protein moves into or near the nucleus toward the end of the G2 phase and reaches its maximum concentration at the G2/M phase junction. Cyclin B1 is degraded during the M phase. The stain

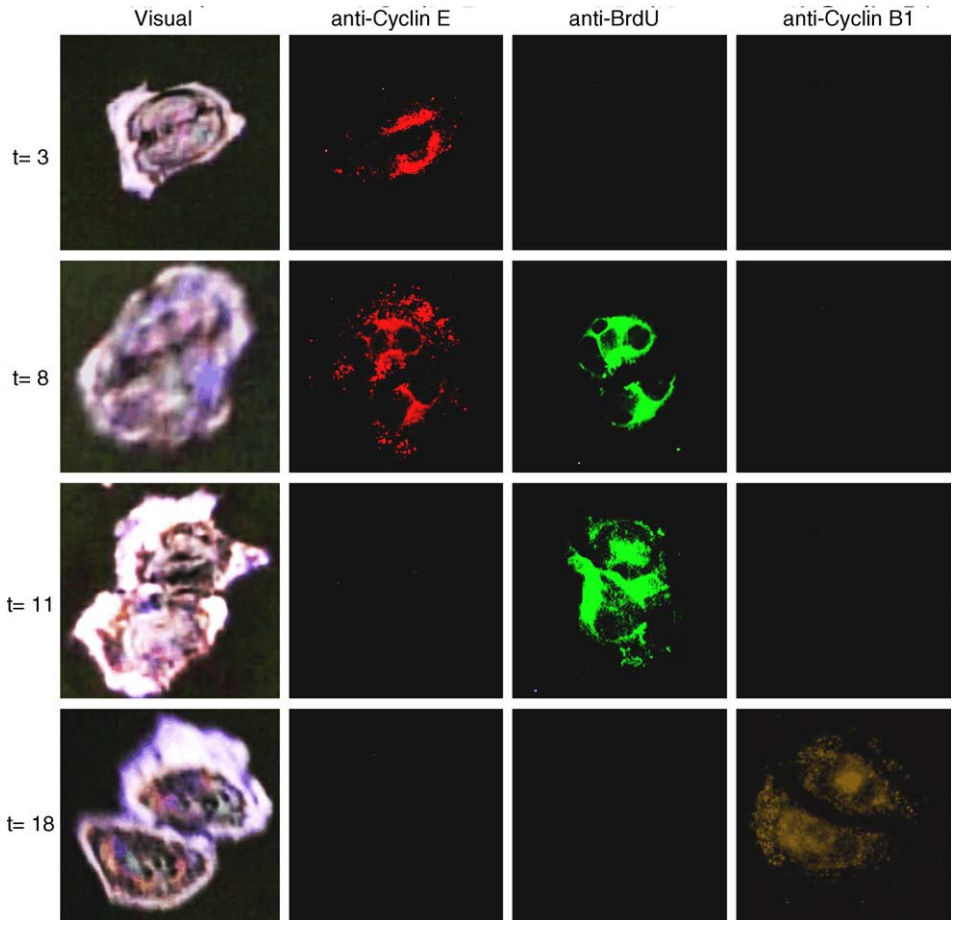

Fig. 3. HeLa cell pairs at incubation times 3, 8, 11 and 18 h post-mitosis. Visual: visual image of the cell pair as seen under the Perkin-Elmer microscope. Anti-cyclin E: result of labeling the cell pairs with anti-cyclin E antibody conjugated with a fluorecent dye. Anti-BrdU: result of labeling the cell pairs with anti-BrdU antibody conjugated with a fluorecent dye. Anti-cyclin B1: result of labeling the cell pairs with anti-cyclin B1antibody conjugated with a fluorecent dye. Each frame is about 70 μm × 70 μm.

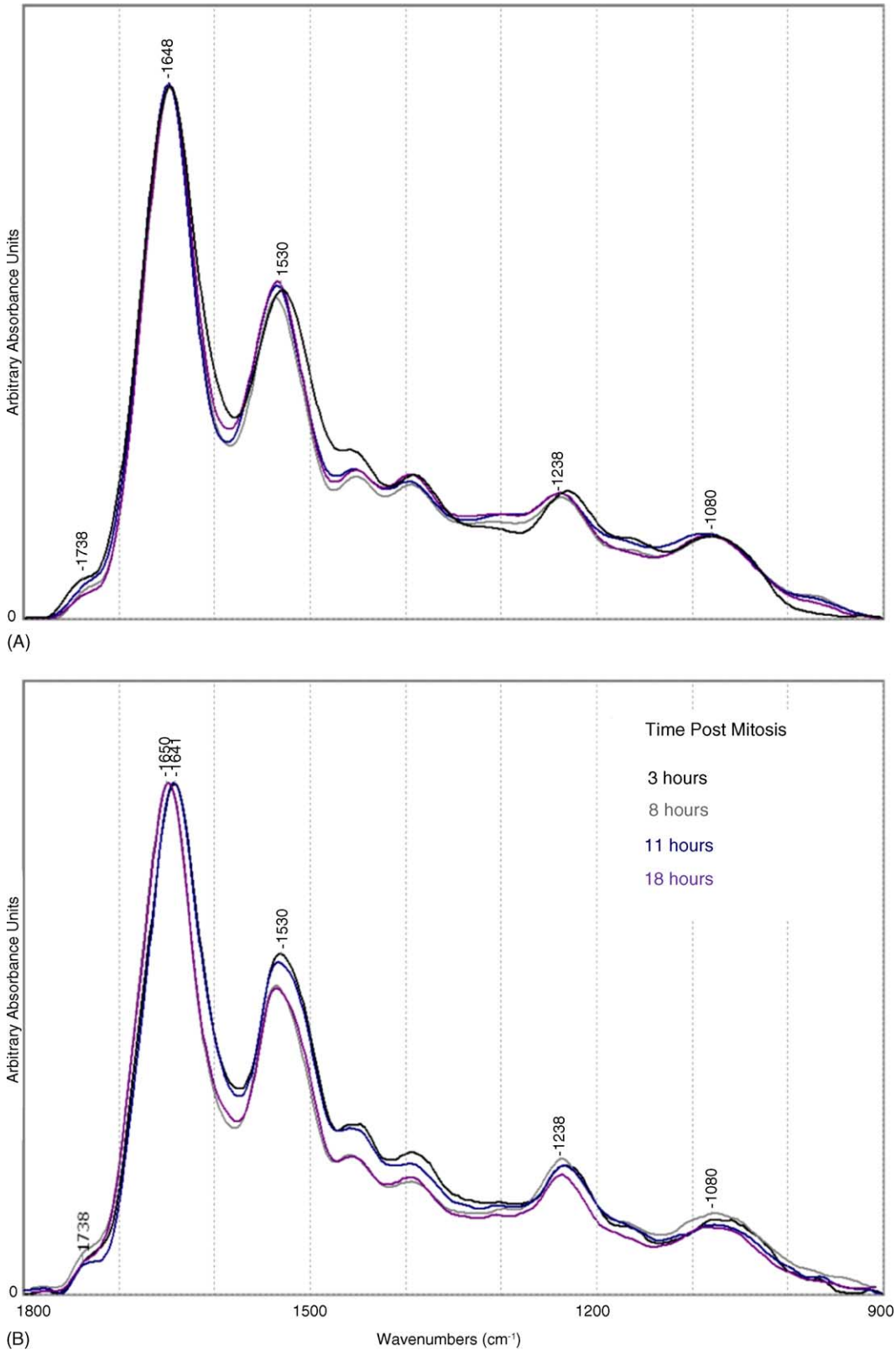

Fig. 4. Overlay of the average FTIR absorption spectra of HeLa cells for time periods 3, 8, 11 and 18 h incubation post-mitosis. (A) Spectra of the entire HeLa cell. (B) Spectra of just the HeLa cell nuclei.

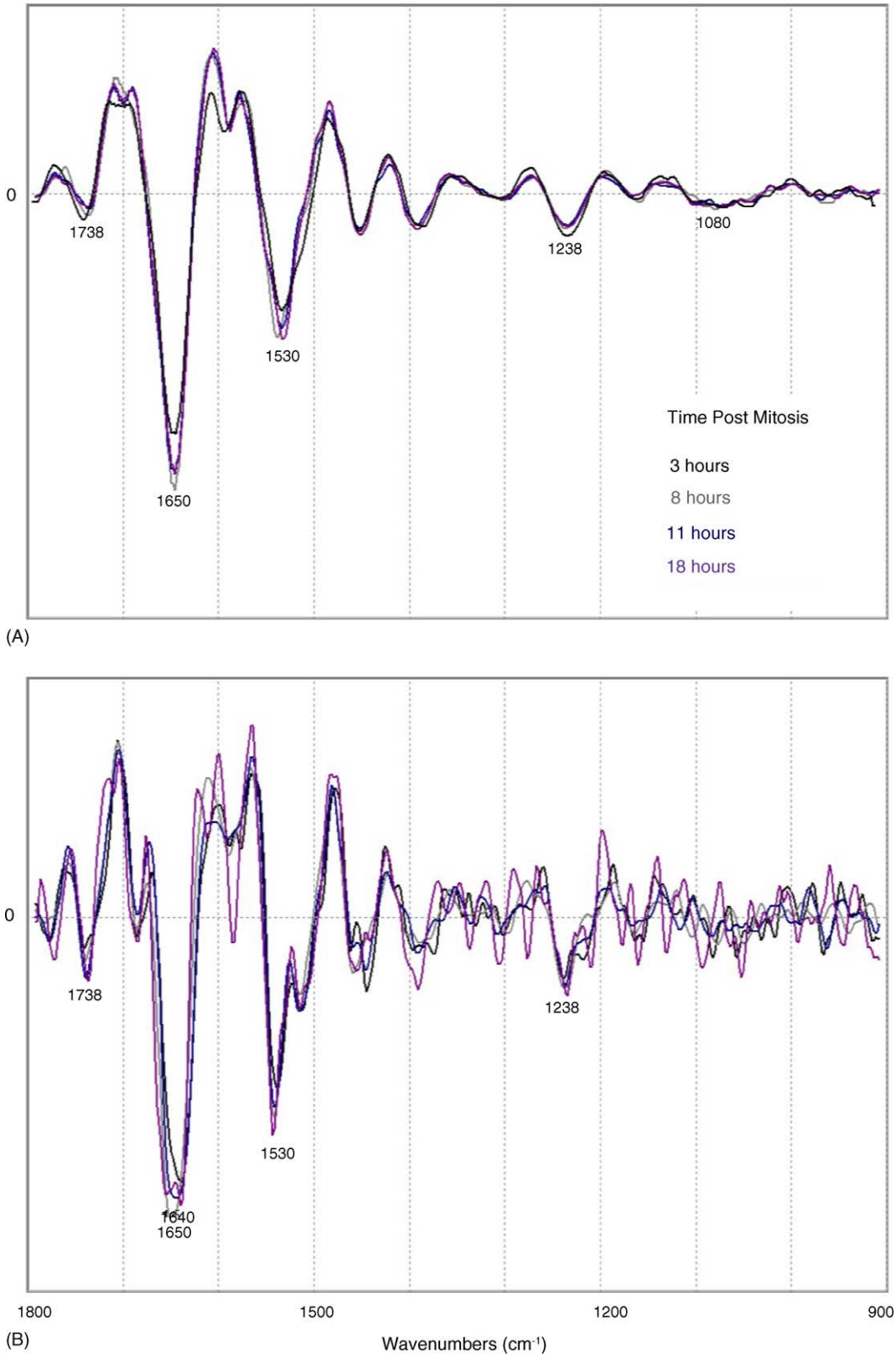

Fig. 5. Overlay of the average second derivative of the FTIR absorption spectra of HeLa cells for time periods 3, 8, 11 and 18 h incubation post-mitosis. (A) Second derivative spectra of the entire HeLa cell. (B) Second derivative spectra of just the HeLa cell nuclei.

response and an assignment in terms of the cell cycle stage are summarized in Table 1.

In Fig. 3, at 3 h incubation post-mitosis, the positive staining for cyclin E and negative staining result for both BrdU and cyclin B1 indicates that the cells were in G1 phase at the time of fixation. At 8 h incubation post-mitosis, the positive green and the positive red staining indicates that the cells were actively synthesizing DNA, yet still contained a significant quantity of cyclin E for detection at the time of fixation. This indicates that these cells were in an early stage of the S phase. By 11 h incubation post-mitosis a negative staining result for both cyclin E and cyclin B1, but positive staining for BrdU suggests that cyclin E has been degraded, DNA is being actively synthesized, yet cyclin B1 has yet to be synthesized. This indicates that the cells are in mid-to-late S phase at the time of fixation. By 18 h incubation post-mitosis, the negative staining result for both cyclin E and BrdU, but positive staining for cyclin B1 suggests that no DNA is being synthesized and no cyclin E remains. We conclude that these cells are in the G2 phase.

Fig. 4 depicts the comparison of the average FTIR absorption spectra of the entire HeLa cells (Panel A) for each of the four elapsed time periods post-mitosis, whereas Panel B shows a comparison of the spectra of the cell nuclei only. All spectra are plotted in the range of 1800–900 cm^{-1}, normalized to the amide I band (~1645 cm^{-1}) absorption intensity.

Fig. 5 shows the comparison of the corresponding second derivative spectra, which emphasize the differences between nuclear and whole-cell spectra, as well the spectral differences observed for the different time points within the cell cycle. The uniformity seen in Fig. 4A is also seen in Fig. 5A. The heterogeneity seen in Fig. 4B is illustrated even more clearly in the second derivative, as seen in Fig. 5B. The nuclear spectra exhibit significant heterogeneity the amide I (~1645 cm^{-1}) and amide II (~1540 cm^{-1}) regions, as well as marked differences in the low frequency (1200–1000 cm^{-1}) region. Our results confirm our previous finding that DNA is barely detectable in the absorption spectra of cells in the G1 and G2 phases of the cell cycle, probably due to its very high optical density. As we expected, the greatest heterogeneity among the spectra of cells of similar biochemical age was found in cells in the S phase. Spectra of cells in the S-phase may or may not exhibit significant spectral contributions of DNA; apparently due to the status of DNA replication.

Table 1
Tabulated results of the immunohistochemical staining of the cell populations at times 3, 8, 11 and 18 h incubation post-mitosis

Time post-mitosis (h)	Cyclin E	BrdU	Cyclin B1	Cell-cycle phase assignment
3	+	−	−	G1
8	+	+	−	Early S
11	−	+	−	Mid or late S
18	−	−	+	G2

The cell pairs were judged either positive or negative for cyclin E, BrdU and cyclin B1. Given the results, the populations were assigned to their respective cell-cycle phases.

4. Discussion and conclusions

In this study, we report for the first time the spectra of cells for which the stage within the cell cycle is known unambiguously. We also have recorded Raman spectra and spectral maps of cells within the stages of mitosis (metaphase, telophase, etc.) at much higher spatial resolution (~1 μm)[12]. The combination of these studies yields a complete spectral characterization of the events that occur during a complete cell cycle.

Inspection of the spectral features at 3, 8, 11 and 18 h time points post-mitosis of the cell cycle reveals, in general, relatively minor changes of the spectral features of these large epithelial cells, both in the original spectra as well as in the second derivative spectra. This indicates that over the entire area of the cell (typically around 3000 μm^2), the much more pronounced changes that occur in the nucleus (<300 μm^2 cross section, see below) are averaged to the point where they can scarcely be detected. However, we notice that these cervical cells, even when actively proliferating, have quite different spectra from those of other cells, such as fibroblasts, for which much larger RNA and phospholipid contributions were observed. In studies carried out on normal (non-malignant) human skin and rat liver fibroblasts, we do observe broad and very intense peaks at ca. 1078 and 1238 cm^{-1}, which were assigned to be due to the phosphodiester species of RNA, DNA and phospholipids. This assignment was confirmed by treatment of the cells with both ethanol (to reduce phospholipid contributions) and ribonuclease, to remove cytoplasmic and nuclear RNA [13]. An indicator of cell proliferation, observed after removal of phospholipids and RNA, was consequently assigned to be due to DNA [14]. Thus, it appears that different cell types give quite different spectra; in particular, it appears that epithelial cells, such as oral mucosa and cervical cells, have particularly low phosphodiester contributions. This is also in agreement for our very earliest reports on cell-cycle-dependent spectral changes on myeloid leukocytes. For these cells, we have previously reported larger spectral differences between cells at different time points of their cell cycle stage in the phosphate spectral region [5]. These cells had much larger nucleus to cytoplasm ratio, and virtually no cytoplasm; thus, the spectral changes are expected to be much larger. However, in these earlier studies, cells were separated by the physical method of centrifugal elutriation into fractions by size and density. Although the fluorecence-activated cell sorting (FACS) analysis determined the approximate cell-cycle phase of the majority of the cells in each elutriated fraction, the exact stage of an individual cell studied by IR microspectroscopy could not be established unambiguously.

For the full-cell spectra of the HeLa cells, the differences at the various time points of the cell cycle manifest themselves mainly in different amide II frequencies, and a small wavenumber shift in the phospholipid peak at 1738 cm^{-1}, mostly between the G1 and the other stages. The cell nuclei, on the other hand, show more pronounced changes between the cells at different time points of the cell cycle (Fig. 4B); these changes are even more evident in the second derivative spectra, Fig. 5B. There are large shifts in the amide I peak position, indicative of different protein structures [15,16] found in the nucleus at different time points [17,18]. Furthermore, the amide II peak is broader in the nucleus, and shows a distinct low frequency shoulder (ca. 1500 cm^{-1}) which is barely evident in the full-cell spectra. This shoulder of the amide II peak also appears to be the most sensitive indicator of the cell's "biochemical age" (time after mitosis), since it is nearly absent in the 18 h-old cells. Finally, DNA peaks (at 1238 and 970 cm^{-1}) are observed in the spectra of the nuclei, particularly in the S-phase spectra.

The frequency range between 900 and 1300 cm^{-1} shows very rich second derivative spectra for the nuclei. We do not believe that these features are due to noise (this spectral range is particularly good in the Perkin-Elmer Spotlight 300 spectrometer), and it is unlikely that the noise between 900 and 1300 cm^{-1} would be much larger than in the amide I/II region. We have seen the rich spectral pattern in the second derivative region in this frequency range before [19] with distinct peaks at about 1035, 1065, 1080, 1105, 1125, 1165 and 1220 cm^{-1}. Furthermore, we have observed differences in these spectral patterns in actively growing and growth inhibited cells. The spectral features coincide with known frequencies of DNA, RNA and phospholipids; however, it is probably not appropriate to attempt to interpret these spectra in detail, given the enormous complexity of the molecules found in a cell's nucleus during cell division. However, we believe that these signals are sensitive indicators of cellular activity.

References

[1] D.N. Wheatley, Cell growth and division, in: The Institute of Biology's Studies in Biology, no. 148, E. Arnold, London, 1982, p. 57.

[2] R. Baserga, The Biology of Cell Reproduction, xi, Harvard University Press, Cambridge, MA, 1985, p. 251.

[3] T.A. Brown, Molecular Biology Labfax, Labfax Series, 2nd ed., Academic Press, San Diego, 1998.

[4] P. Lasch, et al. Infrared spectroscopy of human cells and tissue: detection of disease, Technol. Cancer Res. Treat. 1 (1) (2002) 1–7.

[5] S. Boydston-White, et al. Infrared spectroscopy of human tissue. V. Infrared spectroscopic studies of myeloid leukemia (ML-1) cells at different phases of the cell cycle, Biospectroscopy 5 (4) (1999) 219–227.

[6] G.F. Merrill, Cell synchronization, Meth. Cell. Biol. 57 (1998) 229–249.

[7] T. Terasima, L.J. Tolmach, Changes in X-ray sensitivity of HeLa cells during the division cycle, Naturwissenschaften 190 (1961) 1210–1211.

[8] J.A. Aten, et al. DNA double labelling with IdUrd and CldUrd for spatial and temporal analysis of cell proliferation and DNA replication, Histochem. J. 24 (5) (1992) 251–259.

[9] H.G. Gratzner, Monoclonal antibody to 5-bromo- and 5-iododeoxyuridine: a new reagent for detection of DNA replication, Science 218 (4571) (1982) 474–475.

[10] I.S. Scott, et al. A novel immunohistochemical method to estimate cell-cycle phase distribution in archival tissue: implications for the prediction of outcome in colorectal cancer, J. Pathol. 201 (2) (2003) 187–197.

[11] A. Koff, et al. Human cyclin E, a new cyclin that interacts with two members of the CDC2 gene family, Cell 66 (6) (1991) 1217–1228.

[12] C. Matthaeus, S. Boydston-White, M. Miljkovic, M. Romeo, M. Diem, Raman and infrared micro-spectral imaging of mitotic cells, Biophys. J., submitted for publication.

[13] M. Diem, L. Chiriboga, H. Yee, Infrared spectroscopy of human cells and tissue. VIII. Strategies for analysis of infrared tissue mapping data and applications to liver tissue, Biopolymers 57 (5) (2000) 282–290.

[14] A. Pevsner, M. Diem, IR spectroscopic studies of major cellular components. III. Hydration of protein, nucleic acid, and phospholipid films, Biopolymers 72 (4) (2003) 282–289.

[15] L.P. Choo, M. Jackson, H.H. Mantsch, Conformation and self-association of the peptide hormone substance P: Fourier-transform infrared spectroscopic study, Biochem. J. 301 (Pt 3) (1994) 667–670.

[16] M. Jackson, H.H. Mantsch, The use and misuse of FTIR spectroscopy in the determination of protein structure, Crit. Rev. Biochem. Mol. Biol. 30 (2) (1995) 95–120.

[17] G.C. Mueller, Biochemical events in the animal cell cycle, Fed. Proc. 28 (6) (1969) 1780–1789.

[18] A. Van Hooser, et al. Histone H3 phosphorylation is required for the initiation, but not maintenance, of mammalian chromosome condensation, J. Cell Sci. 111 (Pt 23) (1998) 3497–3506.

[19] A. Pacifico, Infrared spectroscopy of cultured cells II. Spectra of exponentially growing, serum-deprived and confluent cells, Vibrat. Spectrosc. 32 (2003) 107–115.